

Quantitative evaluation of wavelet based image processing algorithms

Zhenxue Jing^{1,2}
Yisheng Zheng³
Walter Huda,^{1,2}
Andrew Laine,³
Jian Fan,³
Yunong Xing⁴

University of Florida, Departments of ¹Nuclear Engineering Science, ²Radiology, ³Computer and Information Sciences, and ⁴Electrical Engineering, Gainesville, Florida 32610

ABSTRACT

Wavelet analysis is currently being investigated as an image enhancement tool for use in mammography. Although this approach to image processing appears to have great promise, there remain major uncertainties regarding an optimal form of wavelet based algorithms. It is, therefore, desirable to have a quantitative method for evaluating a wavelet based image processing algorithm. Optimization of algorithms *prior* to evaluation using standard Receiver Operating Characteristic (ROC) methods is made possible.

A mathematical method has been developed where the input signal is a gaussian with added random noise. An enhancement factor (EF) is obtained from input and output signal-to-noise ratios, SNR_i and SNR_o , ($EF = SNR_o / SNR_i$). The development and testing of this method is described, and a practical application is given showing the major features of a wavelet based image processing algorithm based on the Frazier-Jawerth transform.

Key words: Mammography, wavelets, image processing, image quality, signal-to-noise ratio, image enhancement

1. INTRODUCTION

Mammography is the most reliable method for early detection of nonpalpable breast cancer.¹ Objects of diagnostic interest include tumors which differ from normal tissue by very small amounts, or microcalcifications which are very small. The resultant low visibility of these objects in the mammograms makes accurate cancer diagnosis problematical.² Digital enhancement of mammograms, together with the use of workstations using computer aided diagnosis tools, may permit a more confident interpretation of difficult cases without resorting to follow-up patient examinations.³ Furthermore, the large number of negative biopsies encountered in current practice may also be reduced if an enhanced mammogram was able to provide a more certain diagnosis.⁴

Conventional image processing techniques generally do not perform well on mammographic images.⁵ Large variations in feature size and shape limit the effectiveness of classical fixed neighborhood techniques such as unsharp masking.^{6,7} The use of processing algorithms based on the wavelet transform has recently been proposed for use in mammography.^{8,9,10,11} This approach to image enhancement is promising because it uses methods similar to those used in the human visual system.^{10,12} In this paper, we develop a mathematical model to investigate the behavior of a wavelet algorithm based on the Frazier-Jawerth Transform (FJT).^{13,14}

2. METHOD

2.1. Mathematical model

Two-dimensional mathematical phantom images were generated which contained a gaussian signal and random noise. Each phantom image consisted of a 512^2 matrix with each pixel coded using 1 Byte, permitting the display of 256 gray levels. A two-dimensional gaussian shape signal was generated with a maximum intensity of I and a full width tenth maximum (FWTM) of W . The location of the signal was at the center of the image.

Random background noise, N , with a gaussian distribution (σ) about the mean (μ), was generated using the expression

$$N = (-2\sigma \ln Y)^{1/2} \cdot \cos(\theta) + \mu \quad (1)$$

where Y is a random variable between 0 and 1, and θ is a random variable between 0 and 2π .¹⁶ Figure 1a shows a profile through the central axis of a phantom image with a FWTM equal to 10 pixels and intensity I equal to 70, and Figure 1b shows a profile through random noise remote from this gaussian signal.

The signal S is the mean value of the signal intensity above the mean background level, where the signal was averaged over the FWTM width W . The noise is the standard deviation, σ , of random fluctuations obtained from a profile taken at a location remote from the signal region. To evaluate improvements from the image processing algorithms investigated, an EF was defined by the expression

$$EF = \frac{SNR_o}{SNR_i} \quad (2)$$

where SNR_i and SNR_o are the input and output signal-to-noise ratios, respectively.

2.2. Wavelet algorithm

The algorithm evaluated in this study is based on the FJT.^{13,15} The inner product of the signal (S) with a wavelet (ϕ) reflects the character of S within the time-frequency region where ϕ is localized. Provided ϕ is spatially localized, two-dimensional features such as shape and orientation are preserved in transform space and may thus be used to characterize features through scale space.

For an isotropic function, a multiresolution representation divides the frequency spectrum of an image x into a low-pass sub-band image y^L and a set of band-pass sub-band images y^L , $L = 1, \dots, M$ where M denotes the number of levels. With a 512 matrix size, the number of levels is 8. If F^L is the equivalent filter for the L th level, $W_L[x]$ denotes the operation of filtering x , and the sub-band image of an L -level multiresolution decomposition is given by

$$y^L = W_L[x] \quad (3)$$

The FJT results in a multiresolution decomposition of the input image at each level L , where maxima of the wavelet coefficients may be determined.¹⁴ Maxima above some threshold value T are multiplied by a selected gain factor, G , followed by the inverse transform to generate the processed image.

The FJT image processing algorithm has three parameters whose values are selected by the operator: (1) level(s) ($L = 1$ through $L = 8$) at which the modifications to the wavelet coefficients are to be performed, with $L = 1$ corresponding to the highest spatial frequencies and $L = 8$ to the lowest (DC cap); (2) the threshold value T above which wavelet coefficients are modified; and (3) the gain factor, G , by which selected wavelet coefficients (i.e. those corresponding to local maxima and above the threshold value T) are to be multiplied. The significance of each of these three parameters was systematically investigated using the mathematical phantom model described above.

3. RESULT AND DISCUSSION

3.1. Optimization strategy

The wavelet based image processing algorithm has three parameters: Level (L), Threshold (T) and Gain (G). In addition, the image signal and noise parameters could also be varied. For the purposes of this study, the noise level was fixed with a mean value of 10 and with a standard deviation of 4. The peak signal intensity was fixed at a value 70 above the mean noise level, but five values of the signal width (W pixels) were investigated (4, 6, 10, 20 and 40).

The initial parameter investigated was L using constant values of $T = 5$ and $G = 10$. For each signal width, there is an optimal value of L which yields the highest EF. The optimal L value for each width was employed in subsequent investigations of the T/G parameters. The next parameter to be studied was T , and the value observed to yield the highest EF was used when investigating the G parameter. Although this method does not guarantee that the final algorithm parameters yields the best possible EF value for this image, the significance and relative importance of each parameter can be investigated.

3.2. L parameter

Figure 2 shows results obtained for the EF vs. L experiments as the width of the gaussian (W) was systematically varied. The optimal value of L increased with increases in the W value which is to be expected. As the level L increases, this corresponds to lower spatial frequencies, and thus the larger objects are located at the levels (frequency bands) corresponding to large L values. The optimal L was 3 for $W = 4$, increasing to 6 for $W = 40$. The absolute value of the EF was about 4 for the narrow gaussian signals ($W = 4, 6$ and 10), but fell to about 2 for the wider gaussian signals ($W = 20$ and 40).

3.3. T parameter

Figure 3 shows the corresponding results obtained of the EF vs. T experiments. As expected, the value of EF approaches 1 when a high threshold is set, since this would exclude all the wavelet coefficients from being modified, and the processed image would then be identical to the original image. For smaller phantoms, the setting of a threshold is clearly important and increases the EF value. This behavior is expected since there is a significant amount of noise at the lower levels which corresponds to the higher frequencies. This also explains the absence of any effect of the threshold for the wider signals where the enhancement of coefficients occurs at higher L values since noise is primarily a high frequency phenomenon.

3.4. G parameter

Figure 4 shows the EF variation with G for each width of the gaussian signal. In each case, images were processed using the values of L and T that yielded the highest EF values. The narrowest signal appears to reach a plateau value (~ 12), but all the other signals show a monotonic increase in the EF value as G increases. The maximum value of EF observed was in excess of 30, suggesting that the output signal-to-noise ratio may be significantly increased by the use of an optimized wavelet based image processing algorithm.

Figure 5 shows profiles through the gaussian signal with a W value of 10 processed with increasing values of the G parameter. As G increases, the noise is reduced throughout the image, and it is seen that there is an overshooting at the edge of the signal. The FJT algorithm enhanced edges by subtracting from the edge its second derivative, thus producing the overshooting observed in Figure 5.

4. CONCLUSIONS

1. The enhancement factor, given by the ratio of the output to input signal-to-noise ratios, can measure the performance of an image processing algorithm.
2. Choices for values of the L, T, and G parameters of the FJT wavelet algorithm have a marked impact on image processing performance.
3. Optimal values of the three parameters defining the image processing algorithm are a function of the width of the input gaussian signal.
4. Optimized algorithms suppress random noise and markedly enhance the visibility of the signal.
5. Optimized algorithms can achieve an improvement as high as 30 in the processed signal-to-noise ratio.

5. ACKNOWLEDGEMENTS

The authors wish to thank Drs. Janice C. Honeyman, Edward V. Staab, and Barbara G. Steinbach for their assistance in this research project and Mrs. Linda Waters-Funk for preparation of the manuscript. Valuable discussions with Sergio Schuler are also acknowledged.

This work was sponsored in part by the Whitaker Foundation and the U.S. Army Medical Research and Development Command, Grant No. DAMD 17-93-J-3003.

6. REFERENCES

1. Feig SA and Hendrick ER. "Risk, benefit, and controversies in mammographic screening," Technical Aspects of Breast Imaging, Haus AG, Yaffe MJ (eds), Radiological Society of North America (RSNA), Oak Brook, pp. 119-135, 1993.
2. Vyborny CJ, Schmidt RA. "Mammography as a radiographic examination: an overview," *RadioGraphics* Vol. 9, pp. 723-764, 1989.
3. Giger ML, Doi K, MacMohan H, et al. "An 'intelligent' workstation for computer-aided diagnosis," *RadioGraphics* Vol. 13, pp. 647-656, 1993.
4. Hendrick ER, Parker SH. "Stereotaxic imaging," Technical Aspects of Breast Imaging, Haus AG, Yaffe MJ (eds), Radiological Society of North America (RSNA), Oak Brook, pp. 257-269, 1993.
5. Morrow WM, Paranjape RB, Rangayyan RM, Desautels JEL. "Region-based contrast enhancement of mammograms," *IEEE Transactions on Medical Imaging*, Vol. 11, pp. 392-406, 1992.
6. Prokop M, Galanski M, Oestmann JW, von Falkenhausen U, Rosenthal H, Reimer P, Nischelsky J, Reichelt S. "Storage phosphor versus screen-film radiography: effect of varying exposure parameters and unsharp mask filtering on the detectability of cortical bone defects," *Radiology* Vol 177, pp. 109-113, 1990.
7. Higashida Y, Moribe N, Morita K, Katsuda N, Hatemura M, Takada T, Takahashi M and Yamashita J. "Detection of subtle microcalcifications: comparison of computed radiography and screen-film mammography," *Radiology* Vol. 183, pp. 483-486, 1992.
8. Laine A, Song S. "Multiscale wavelet representations for mammographic feature analysis," *Proceedings of SPIE: Conference on Mathematical Methods in Medical Imaging*, San Diego, July 23-25, 1992.

9. Laine A, Song S. "Wavelet processing techniques for digital mammography," Proceedings of SPIE: Conference on Visualization in Biomedical Computing, Chapel Hill, October 13-16, 1992.
10. Laine A, Schuler S, Huda W, Honeyman JC, Steinbach BG. "Hexagonal wavelet processing of digital mammography," Proceedings of SPIE Conference on Medical Imaging VII, Newport Beach, SPIE, Vol 1898, pp. 559-573, 1993.
11. Laine A, Song S, Fan J, Huda W, Honeyman JC, Steinbach BG. "Adaptive multiscale processing for contrast enhancement," Proceedings of the SPIE Conference on Medical Imaging, San Jose, SPIE, Vol. 1905, pp. 521-532, 1993.
12. Wiesel TN. "Postnatal development of visual cortex and the influence of environment (Nobel Lecture)," Nature, Vol. 299, pp. 583-591, 1982.
13. Frazier M, Jawerth B, Weiss G. "Littlewood-Paley theory and the study of function spaces". Conference Board of the Mathematical Sciences. Regional Conference Series in Mathematics, Number 79, 1991.
14. Laine A, Schuler S, Fan J and Huda W. "Mammographic feature enhancement by multiscale analysis," Accepted for publication by IEEE Transactions on Medical Imaging, 1994.
15. Laine A, Ball W and Kumar A. "A multiscale approach for recognizing complex annotations in engineering documents," IEEE Computer Society Conference on Computer Vision and Pattern Recognition, Lahaina, Maui, Hawaii, June 3-6, 1991.
16. Weeks AR, Myler HR and Wenaas HG. "Computer-generated noise images for the evaluation of image processing algorithms," Optical Engineering Vol. 5, pp. 982-992, 1993.

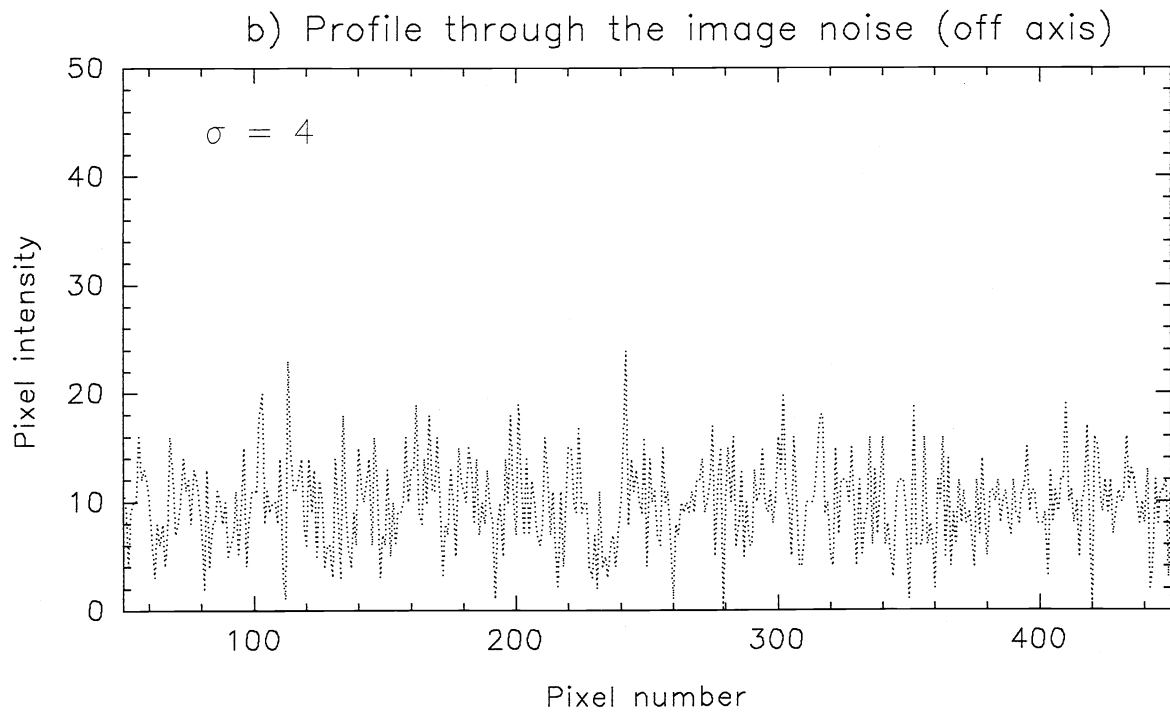
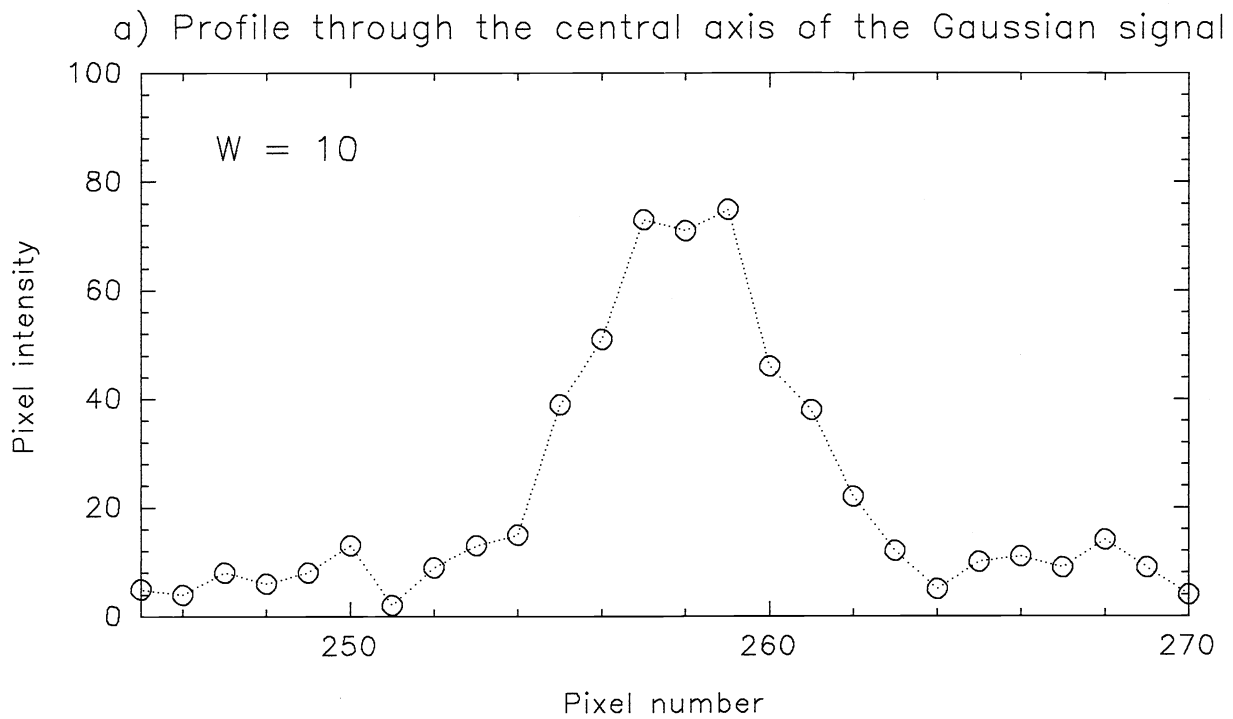


Figure 1

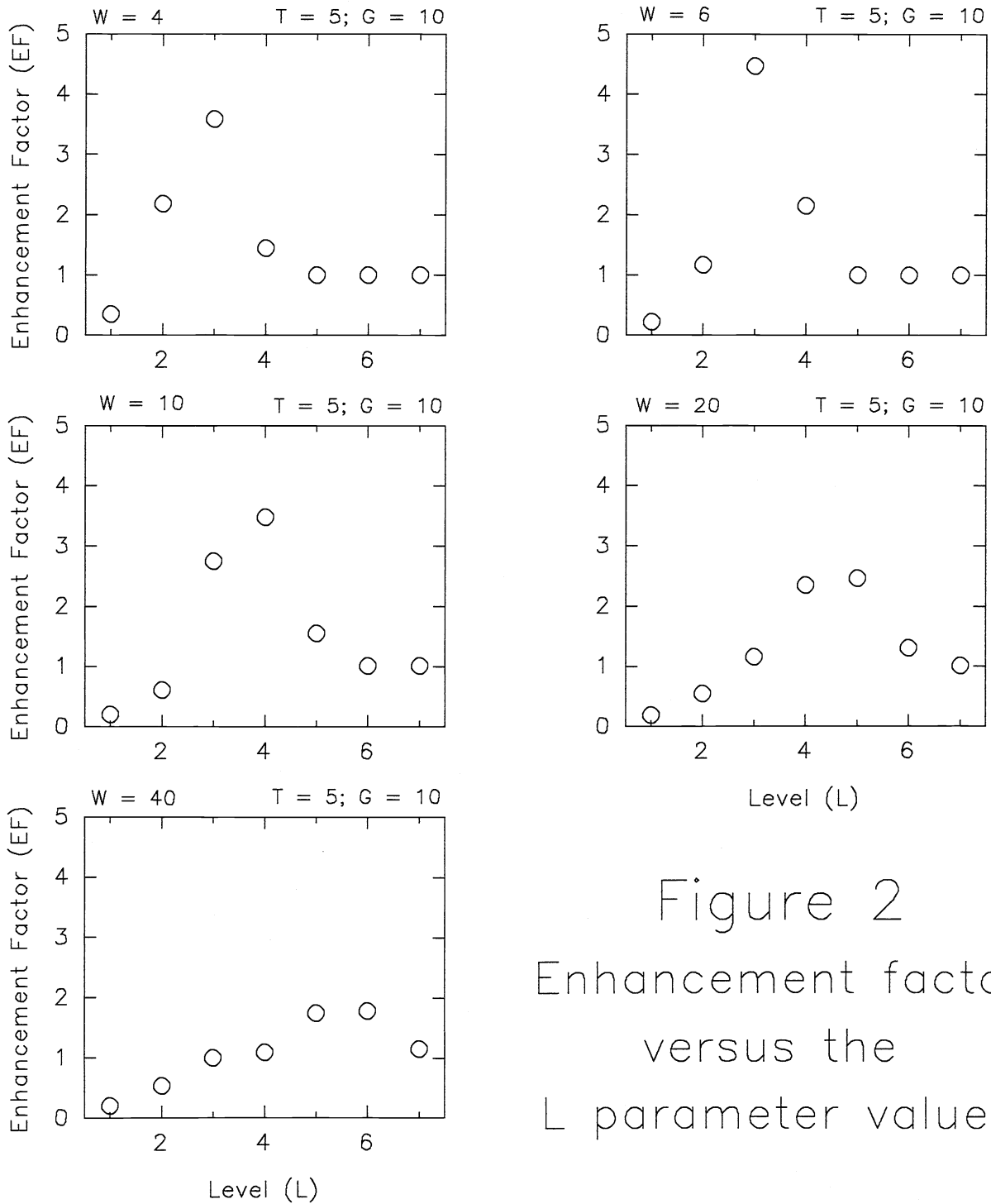
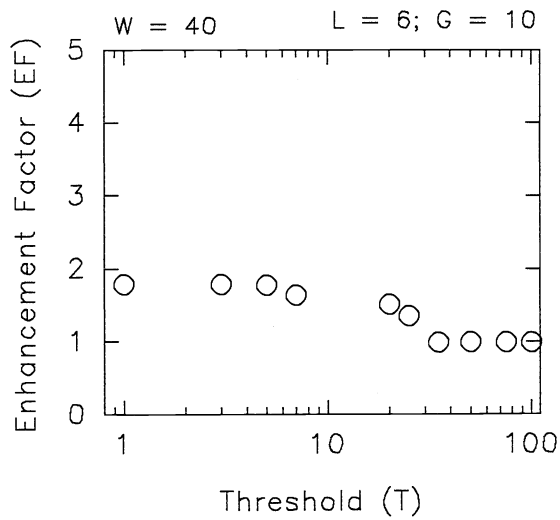
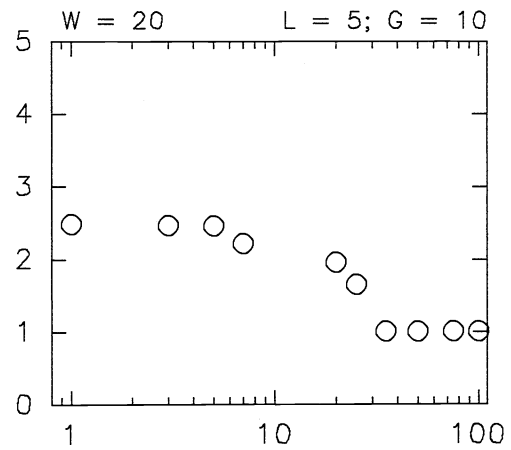
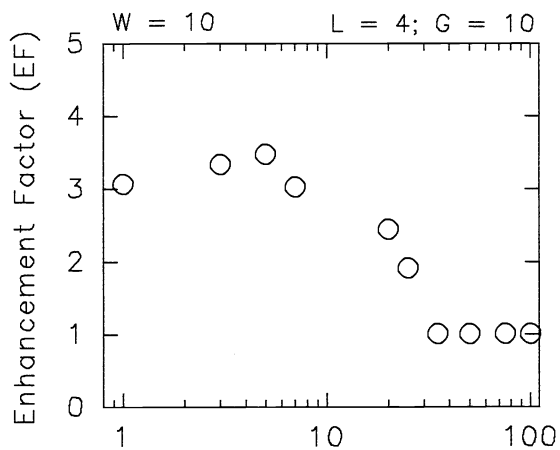
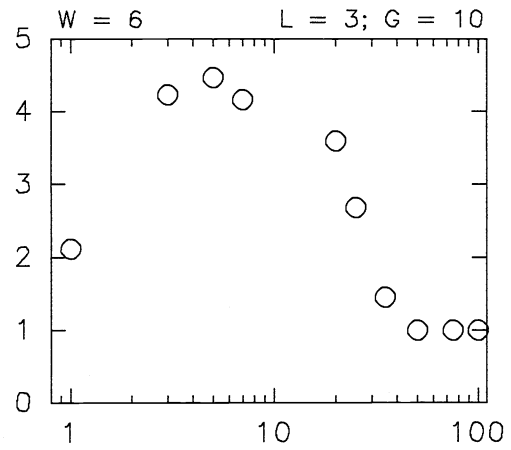
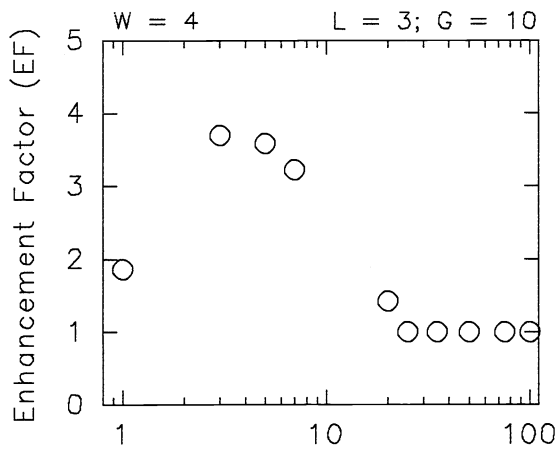
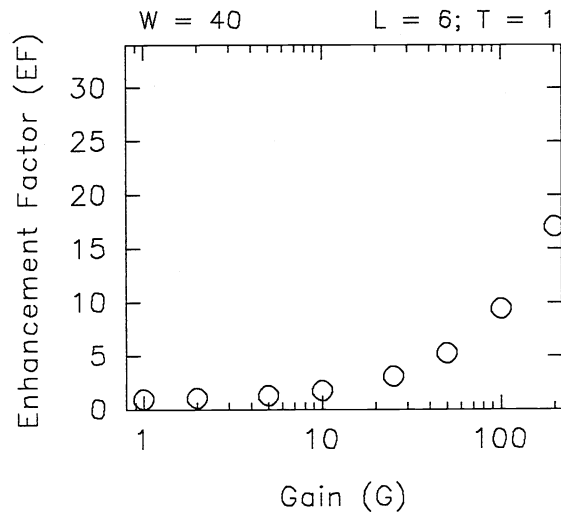
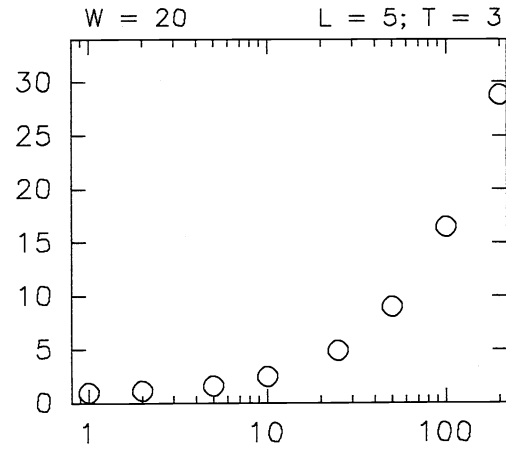
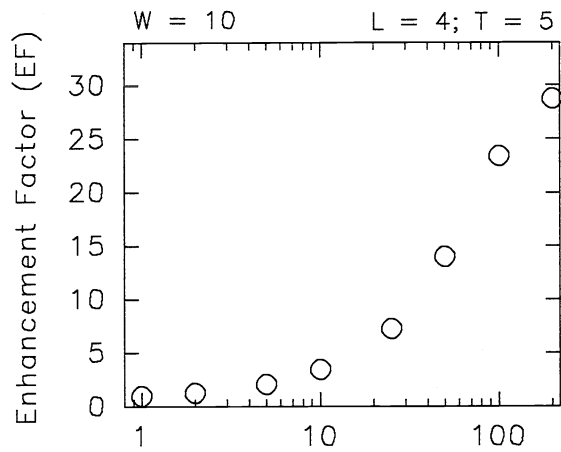
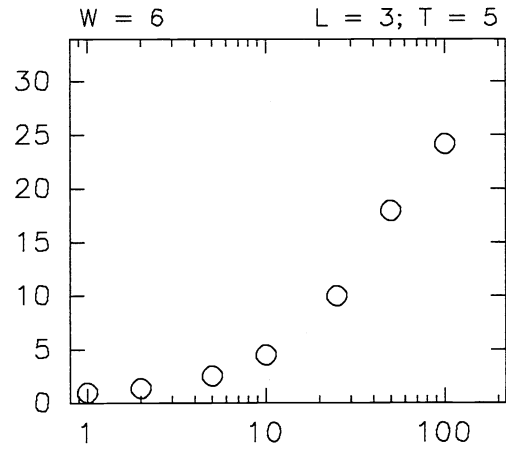
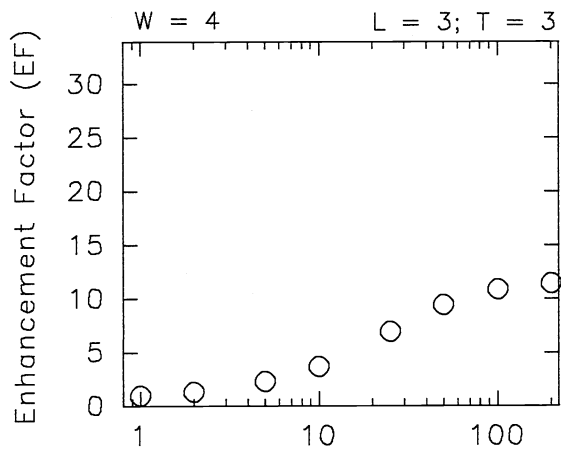


Figure 2
 Enhancement factor
 versus the
 L parameter value



Threshold (T)

Figure 3
Enhancement factor
versus the
T parameter value



Gain (G)

Figure 4
Enhancement factor
versus the
G parameter value

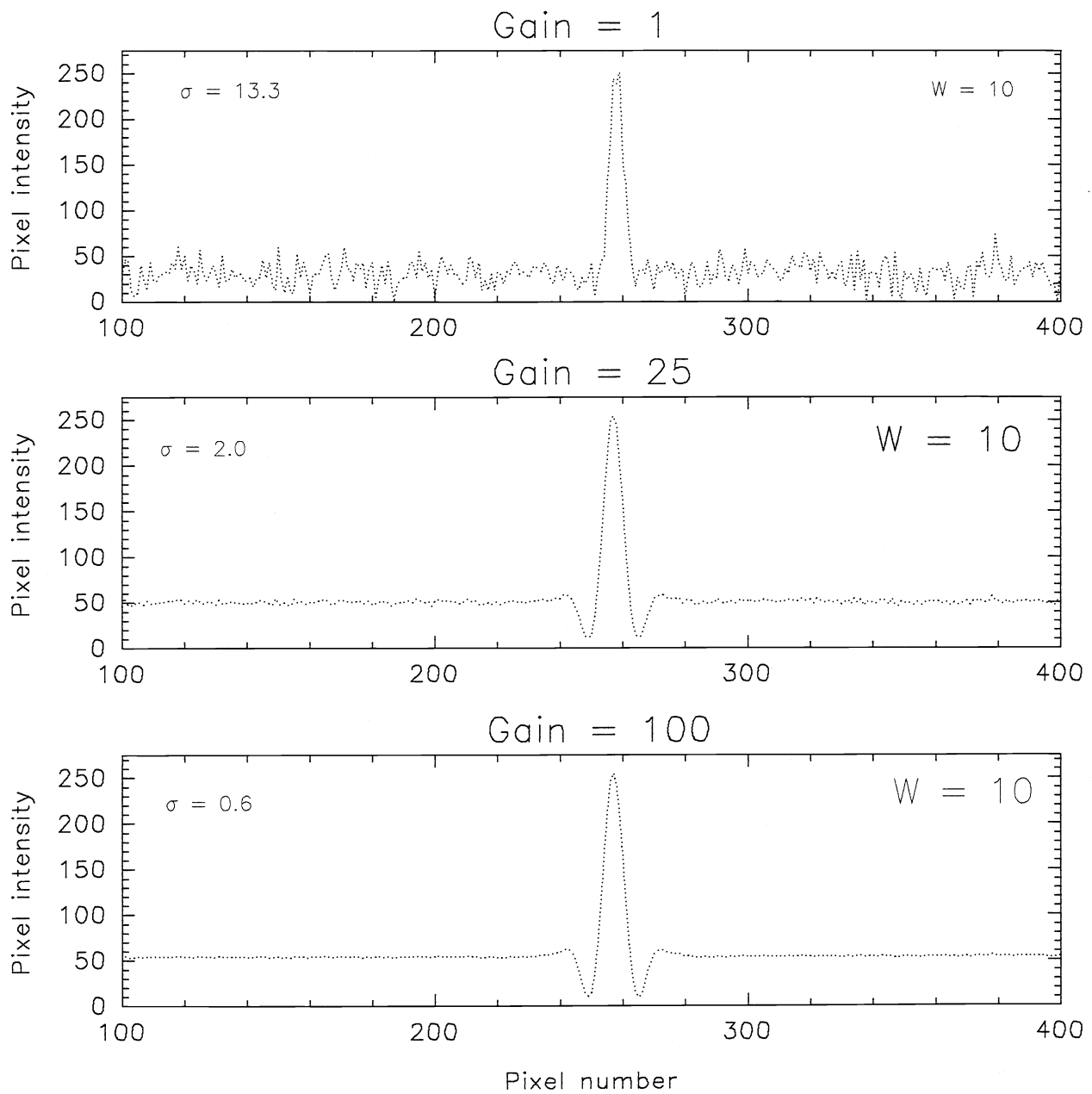


Figure 5
 Profiles through central
 axis of the Gaussian signal